Spreading of a liquid film with a finite contact angle by the evaporation/condensation process

ARTICLE *in* LANGMUIR · JANUARY 1993

Impact Factor: 4.46 · DOI: 10.1021/la00025a056

2 AUTHORS, INCLUDING:

P. C. Wayner
Rensselaer Polytechnic Institute
146 PUBLICATIONS **2,620** CITATIONS

Spreading of a Liquid Film with a Finite Contact Angle by the Evaporation/Condensation Process

Peter C. Wayner, Jr.

The Isermann Department of Chemical Engineering, Rensselaer Polytechnic Institute, Troy, New York 12180-3590

Received August 19, 1992. In Final Form: October 23, 1992

Classical condensation and interfacial concepts like the Kelvin, Young-Dupre, and augmented Young-Laplace equations are used to develop a simple physical model of contact line motion for the finite contact angle case at relatively low velocity. Theoretical predictions of the velocity are compared with experimental data in the literature for the following three significantly different systems: octane on Teflon (apparent contact angle, $\theta_e = 26°$) and methylene iodide on nylon ($\theta_e = 41°$) obtained on flat surfaces and the capillary rise of water in a dehydroxylated glass capillary ($\theta_e = 36°$). The results demonstrate that the evaporation/condensation process could have a significant effect on contact line movement in these systems at 293 K. We also find that the forced increase in the observable apparent contact angle could be an approximate measure of the condensation rate in the vicinity of the contact line and therefore contact line velocity due to condensation.

Introduction

The spreading dynamics of fluids on solid substrates have received considerable attention because of its generic importance in such diverse processes as coating, soldering, lubrication, drying, and thin film change-of-phase heat transfer. The movement of the contact line (three phase line, TPL) at the leading edge of the film is of particular importance because it controls the result of the process. Therefore, a physical model based on intermolecular forces would not only be useful in correlating data but lead to improvements in the wetting process. Herein, we focus on the interfacial physics of a simple condensation model for contact line motion.

Models concerning the spreading of *nonvolatile* liquids are discussed extensively in recent reviews.[1-4] For example, Hansen and Toong[5] and Huh and Scriven[6] demonstrated that classical hydrodynamic concepts failed in the immediate vicinity of the contact line because of the no slip condition. On the other hand, Blake[3] demonstrated that a stress modified molecular rate process[7,8] can account for major features of the moving contact line. Within these types of studies, the question of volatility is usually given secondary importance. However, if the displaced fluid is a gas and the liquid is sufficiently "volatile", the liquid can evaporate upstream from the thicker portion of the contact line region and condense where necessary to help relieve the resistance to motion in the contact line region where the film thickness is extremely thin. This was suggested in the pioneering experimental results of Hardy and Doubleday,[9] Bangham and Saweris,[10] and Bascom et al.[11] More recently, Wayner[12] theoretically demonstrated that evaporation/condensation should be an important mechanism in contact line motion because the potential for flow exists in both the liquid and vapor spaces. This was numerically demonstrated for the completely wetting case in ref 13. The objective of this work is to use classical interfacial concepts (the Kelvin, Young-Dupre, and augmented Young-Laplace equations) to develop a simple physical model of contact line motion based on the evaporation/condensation process for the finite contact angle case. Since the thicker portion of the film is relatively very large, sufficient area for evaporation is always present. Therefore, the condensation process is emphasized. Since the distances are extremely small, large mass fluxes in the vapor and large heat fluxes in the solid are easily possible with small differences in the vapor pressure and temperature. Briefly, we propose that a forced increase in the apparent (macroscopically measured) contact angle gives an increase in the curvature (or its equivalent) in the immediate vicinity of the contact line. This leads to a local decrease in the vapor pressure and condensation with contour movement as expected from the Kelvin equation. Although this model is developed herein for the finite angle system, the results could be used to extend the modeling in ref 13 for the completely wetting system.

The model is based on a simple microscopic thermodynamic description of the interfacial profile in the contact line region which agrees with the Young-Dupre equation and macroscopic observations for both the horizontal and vertical cases. Wayner[14] demonstrated that the augmented Young-Laplace equation for the equilibrium case could be solved for the details of the profile. The results presented in ref 14 added detail to White's[15] conceptual view of the contact line region which is presented in Figure 1. During the review period, earlier discussions of this view of the contact line region by Broekhoff and de Boer[16] and by Broekhoff[17] were brought to the attention of the author. In these two references, thermodynamic reasoning

(1) Slattery, J. C. *Interfacial Transport Processes*, 1st ed.; Springer-Verlag: New York, 1990.
(2) Brochard-Wyart, F.; de Gennes, P. G. *Adv. Colloid Interface Sci.* **1992**, *39*, 1-11.
(3) Blake, T. D. Presented at the 1988 AIChE Meeting New Orleans, LA, March 1988, Paper 10142.
(4) Cazabat, A. M. *Contemp. Phys.* **1987**, *28*, 347-364.
(5) Hansen, R. J.; Toong, T. Y. *J. Colloid Interface Sci.* **1971**, *37*, 196-207.
(6) Huh, C.; Scriven, L. E. *J. Colloid Interface Sci.* **1971**, *35*, 85-101.
(7) Cherry, B. W.; Holmes, C. M. *J. Colloid Interface Sci.* **1969**, *29*, 174-176.
(8) Blake, T. D.; Haynes, J. M. *J. Colloid Interface Sci.* **1969**, *30*, 421-423.
(9) Hardy, W. R.; Doubleday, I. *Proc. R. Soc. London, Ser. A* **1922**, *100*, 550-574.
(10) Bangham, D. H.; Saweris, Z. *Trans. Faraday Soc.* **1938**, *34*, 554-570.
(11) Bascom, W. D.; Cottington, R. L.; Singleterry, C. R. In *Contact Angle, Wettability and Adhesion*; Gould, R. E., Ed.; Advances in Chemistry Series No. 43; American Chemical Society: Washington, DC, 1964; pp 355-379.
(12) Wayner, P. C., Jr. *Colloids Surf.* **1991**, *52*, 71-84.
(13) Wayner, P. C., Jr.; Schonberg, J. *J. Colloid Interface Sci.* **1992**, *152*, 507-520.
(14) Wayner, P. C., Jr. *J. Colloid Interface Sci.* **1982**, *88*, 294-295.
(15) White, L. R. *J. Chem. Soc., Faraday Trans.* **1977**, *73*, 390-398.
(16) Broekhoff, J. C. P.; de Boer, J. H. *J. Catal.* **1968**, *10*, 391-400.

0743-7463/93/2409-0294$04.00/0

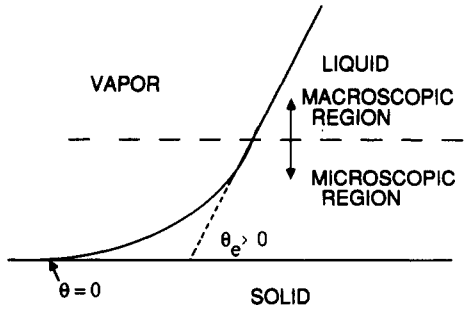

Figure 1. Conceptual view of contact line region given by White.[15]

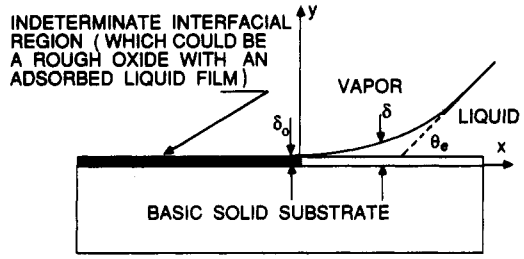

Figure 2. Conceptual view of contact line region with $\delta = \delta_0$ at the leading edge. Additional details are given in Figures 3 and 4 presented in the next section.

led to an extension of the Kelvin equation for both the complete wetting and the finite apparent contact angle cases. Their work followed a seminal presentation by Derjaguin[18] for the case of liquids in capillary pores. Within these analyses, a microscopic real contact angle of zero is consistent with a curved interface and a macroscopic apparent equilibrium finite contact angle, θ_e. In a finite contact angle system, the decrease in equilibrium vapor pressure due to a positive curvature is offset by the effect of "disjoining pressure". Some aspects of this model were discussed in the context of more complicated liquid–solid systems by Brochard-Wyart et al.[19] Adding the concept of the stratified substrate presented in ref 20, the original picture used in ref 14 is redrawn and presented in Figure 2. The important "characteristic thickness" at the leading edge where the slope vanishes is δ_0. Although we view the *exact* nature of the liquid–solid interface to be indeterminate, the *conceptual* ideas of a moist surface like but not restricted to an "ultrathin surface oxide with adsorbed liquid" or "a nonplane surface where extremely small lens of liquid can form" are sufficient for model development. In addition, the details of the diffuse liquid–vapor interface, which can be described by the density gradient concept, are also hidden within this model. However, subsequent calculation of the velocity of the contact line does not depend on an exact visual picture of the surface. *We find the change in the observable apparent contact angle sufficient for this purpose.* Theoretical predictions of the velocity are compared successfully with experimental data for the following three significantly different systems: octane on Teflon (apparent contact angle, $\theta_e = 26°$) and methylene iodide on nylon ($\theta_e = 41°$) obtained on flat surfaces by Schwartz and Tejada[21] and the capillary rise of water in a dehydroxylated glass capillary ($\theta_e = 36°$) obtained by Gribanova.[22] (We note that the sign convention for the Hamaker constant used herein is opposite that used in some references like ref 19. By use of the terminology of ref 19, the "pseudo partial wetting" case is analyzed below.)

Herein and in refs 12, 16, and 17, an extended Kelvin equation for a liquid in equilibrium with its saturated vapor is used in the partial wetting contact line region where the film thickness can be as thin as a monolayer. We know from relatively macroscopic measurements and theory that the curvature and the thickness of a liquid film will each change the stress field and therefore the very dynamic vapor–liquid equilibrium exchange process at the interface. Extrapolation below of these observations to a very small scale at the contact line allows new models (and questions) concerning the region to be discussed. We feel that this extrapolation into a region, which can only be viewed by the resulting apparent contact angle, is probably made valid by the highly dynamic motion of the molecules which must be a function of the local shape (stress field) of the film on the substrate. Conceptually, this stress field is described using "thickness" and "curvature". Some experimental information on the validity of this type of extrapolation has been obtained by Fisher and Israelachvili[23] and by Christenson[24] who demonstrated that the thermodynamic basis of the Kelvin equation is valid in principle for radii as low as 4 nm, which is still larger than some of the systems discussed below. Therefore, final experimental confirmation of this approach awaits a considerable amount of additional study.

Continuum Model Based on Interfacial Thermodynamics

The Gibbs–Duhem equations for the two bulk phases (v, vapor; l, liquid) in the gravitational field presented in Figure 2 are

$$n_v \, d\mu_{vg} = -s_v \, dT + \rho_v g \, dy + dP_v \quad (1)$$

$$n_l \, d\mu_{lg} = -s_l \, dT + \rho_l g \, dy + dP_l \quad (2)$$

$$\mu_g = \mu + Mgy \quad (3)$$

where n = molar density, P = pressure, s = entropy/volume, T = temperature, μ = chemical potential/mol, and ρ = mass density. Taking the difference between eqs 1 and 2 at equilibrium with $\mu_{v_g} = \mu_{l_g}$ gives

$$d\mu_g = \frac{(s_l - s_v)}{(n_v - n_l)} dT + \frac{(\rho_v - \rho_l)}{(n_v - n_l)} g \, dy + \frac{1}{(n_v - n_l)} d(P_v - P_l) \quad (4)$$

We assume that the following augmented Young–Laplace equation gives the difference in the isothermal volumetric chemical potential (which can be viewed as an effective pressure) between the vapor and the liquid

$$P_v - P_l = \Pi + \sigma_{lv} K \quad (5)$$

where P_v is the pressure in the vapor at the liquid–vapor interface, P_l is the pressure in the liquid at the interface, Π is the disjoining pressure, σ_{lv} is the liquid–vapor interfacial free energy, and K is the curvature of the liquid–vapor interface. Combining eqs 3–5 gives for constant temperature

$$(\Delta n) RT \, d \ln f = d(\Pi + \sigma_{lv} K) \quad (6)$$

in which Δn is the molar density difference $(n_v - n_l)$ and

(17) Broekhoff, J. C. P. Adsorption and Capillarity, Pd.D. Thesis, University of Technology, Delft, 1969; pp 92–101.
(18) Derjaguin, B. V. in *Proceedings of the International Congress on Surface Activity, 2nd*; Butterworth: London, 1957; Vol. 2, pp 153–159.
(19) Brochard-Wyart, F.; di Meglio, J. M.; Quere, D.; de Gennes, P. G. *Langmuir* **1991**, *7*, 335–338.
(20) Brochard-Wyart, F.; de Gennes, P. G.; Hervet, H. *Adv. Colloid Interface Sci.* **1991**, *34*, 561–582.
(21) Schwartz, A. M.; Tejada, S. B. *J. Colloid Interface Sci.* **1972**, *38*, 359–375.
(22) Gribanova, E. V. *Adv. Colloid Interface Sci.* **1992**, *39*, 235–255.
(23) Fisher, L. R.; Israelachvili, J. N. *J. Colloid Interface Sci.* **1981**, *80*, 528–540.
(24) Christenson, H. K. *J. Colloid Interface Sci.* **1988**, *121*, 170–178.

R is the gas constant. For convenience, the fugacity, f, will subsequently be replaced by the equilibrium vapor pressure of the film, P_v. Therefore, the vapor pressure is a function of the thickness profile.

Integrating eq 6 at constant liquid molar density ($\Delta n \cong -\rho_{lM}$) between a reference state ($f = P_r$, Π_r, K_r) and a final state P_v, Π, and K gives

$$\rho_{lM} RT \, d \ln \frac{P_v}{P_r} = (\Pi + \sigma_{lv} K)_r - (\Pi + \sigma_{lv} K) \qquad (7)$$

For the horizontal equilibrium case presented in Figure 2, the equilibrium vapor pressure is essentially constant for the contact line region in which the film thickness changes by a very small amount.[14] Therefore, with $P_v = P_r$

$$\Pi + \sigma_{lv} K = 0 \qquad (8)$$

It is important to note that, in this case, the reference vapor pressure is fixed by the closest bulk liquid interface where both K and Π vanish. Equation 8 is the augmented Young–Laplace equation for the equilibrium contact line region. It can also be viewed as an extended Kelvin equation for the equilibrium case.

Using eqs 9, 10, and 11, eq 8 is expanded and made dimensionless to obtain eq 12 for the dimensionless curvature, Ψ

$$K = \frac{d^2\delta}{dx^2}\left[1 + \left(\frac{d\delta}{dx}\right)^2\right]^{-1.5} \qquad (9)$$

$$\Pi = -\frac{\bar{A}}{\delta^3}, \quad \bar{A} = \frac{A_{ll} - A_{ls}}{6\pi} \qquad (10)$$

where δ is the film thickness and $A_{ls} < A_{ll}$ are the Hamaker constants for the liquid–solid and liquid–liquid systems respectively (the partial wetting case with a finite apparent contact angle is emphasized herein). Restrictions on the use of this simple model are discussed in ref 25 for a completely wetting case

$$x = \delta_0 \xi, \quad \delta(x) = \delta_0 \eta(\xi), \quad b = \sigma_{lv} \delta_0^2 / \bar{A}, \quad \frac{d\delta}{dx} = \frac{d\eta}{d\xi}, \quad \frac{d^2\delta}{dx^2} = \frac{d^2\eta}{\delta_0 \, d\xi^2} \qquad (11)$$

$$\Psi \equiv \left[1 + \left(\frac{d\eta}{d\xi}\right)^2\right]^{-1.5} \frac{d^2\eta}{d\xi^2} = [b\eta^3]^{-1} \qquad (12)$$

in which the constant, δ_0, is a characteristic length of molecular size that is used as the effective thickness at the contact line. Ψ is a dimensionless curvature.

Using the substitution $q = d\eta/d\xi$ in eq 12 and the boundary conditions $\eta(0) = 1$ for the dimensionless thickness at the contact line and $q = \eta'(0) = 0$ for a zero slope at the contact line gives

$$\int_0^q \frac{q \, dq}{[1 + q^2]^{1.5}} = \int_1^\eta \frac{d\eta}{b\eta^3} \qquad (13)$$

Equation 13 has been integrated for constant "b" to obtain eq 14 for the cos $\theta_{e\eta}$ where $\theta_{e\eta}$ (η) = arc tan δ' is the local angle at η[14]

$$\cos \theta_{e\eta} = 1 - \frac{1}{2b} + \frac{1}{2b\eta^2} \qquad (14)$$

In the limit of "large" η, the last term on the right-hand side of eq 14 can be neglected and the Young–Dupre equation is obtained[14]

$$\sigma_{lv} \cos \theta_e = \sigma_{sv} - \sigma_{ls} \qquad (15)$$

where the approximation $\sigma_{lv} = 2b(\sigma_{lv} - \sigma_{sv} + \sigma_{ls})$ has been used. It is important to note that the "transition region", where $1/2b\eta^2$ is important, is very small since the characteristic length is of molecular size. Although the effect of the assumption of a constant value for "b" on the details of the film profile has not been completely resolved, the final result agrees with the Young–Dupre equation and the observable contact angle. From eq 8, the following equation can be obtained for the equilibrium curvature at the contact line, K_{eo}, where $\delta = \delta_0$

$$K_{eo} = -\frac{\Pi_o}{\sigma_{lv}} = \frac{1}{b\delta_0} \qquad (16)$$

Within the context of the extended Kelvin model, eq 16 suggests that the film of average thickness δ_0 can be described as numerous small "curved patches" (which could be of molecular size): the reduction in vapor pressure due to curvature offsets the vapor pressure increase due to thickness (disjoining pressure). Since real surfaces are not perfectly flat at least at the molecular scale, these patches (or individual molecules in the limit of very small concentration) could fit in the surface depressions. Conceivably, the contact line connects a series of depressions in which the curved interface fits. We hasten to note that the previous description is possibly only a consistent schematic view.

Equations 12 and 14 are presented in Figures 3 and 4. The value of the constant b can be obtained using $b^{-1} = 2(1 - \cos \theta_e)$.

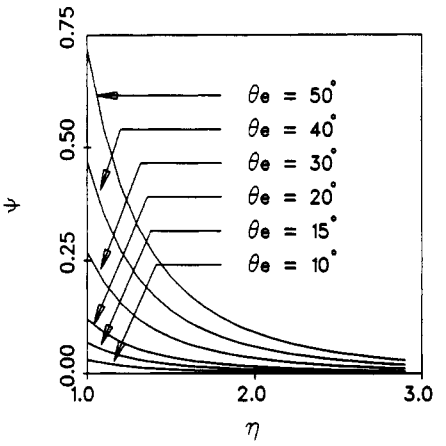

Figure 3. Dimensionless curvature profile obtained using eq 12 with $b^{-1} = 2(1 - \cos \theta_e)$.

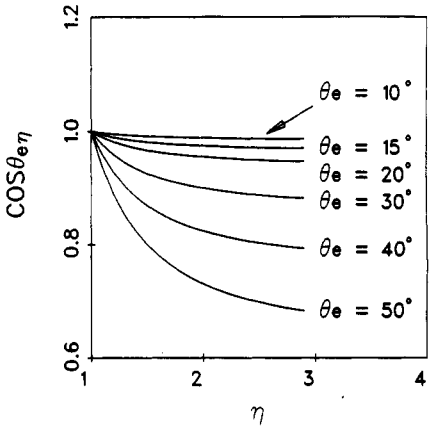

Figure 4. Variation of cos (atan δ') obtained using eq 14 with $b^{-1} = 2(1 - \cos \theta_e)$.

(25) Truong, J. G.; Wayner, P. C., Jr. *J. Chem. Phys.* **1987**, *87*, 4180–4187.

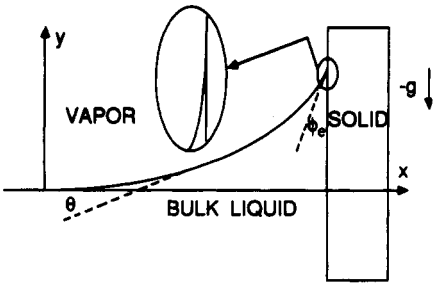

Figure 5. Meniscus formed on a vertical plate immersed in a pool of liquid.

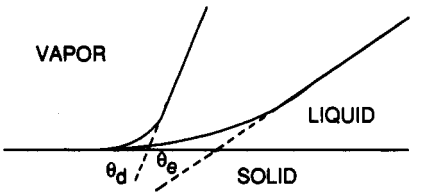

Figure 6. Forced change in profile represented by $\theta_e \rightarrow \theta_d$. The resulting movement is not shown.

The local curvature *outside* the small transition region near the contact line for the *vertical* case presented in Figure 5 is given by eq 17

$$K = \frac{\rho_l g y}{\sigma_{lv}} \tag{17}$$

This has been integrated to obtain[26,27]

$$1 - \sin \phi_e = \frac{\rho_l g y_e^2}{2\sigma_{lv}} \tag{18}$$

The apparent equilibrium contact angle at the height y_e is ϕ_e. Since the characteristics of eq 14 demonstrate that $(2b\eta^2)^{-1}$ becomes unimportant rapidly, eq 17 is a very good approximation (except for the very small region where Π is important) of the complete profile of a meniscus on a vertical surface. Using eqs 17 and 18 gives

$$K^2 = \frac{2\rho_l g}{\sigma_{lv}}(1 - \sin \phi_e) \tag{19}$$

for the curvature near the contact line. Due to the pressure drop in the vertical meniscus and in the vapor, eq 19 demonstrates that the curvature and the apparent contact angle are associated with a change in vapor pressure. Therefore, we can expect that a forced change in the apparent contact angle would be associated with a change in the equilibrium vapor pressure in the curved portion of the meniscus. We note that there is an additional increase in the equilibrium curvature in the vertical case where the apparent contact angle changes to merge with the surface. To obtain the profile in this small region, the reference vapor pressure can be assumed to be constant over this very short distance and equal to the value at y_e.

Rewriting eq 7 for a forced change ($\theta_e \rightarrow \theta_d$) in the profile for the *horizontal* pseudoequilibrium case presented in Figure 6 with $P_r = P_v$ for the thick plane region where $\Pi = 0$ and $K = 0$, and $P_v = P_{vd}(x)$ for the rest of the changed interface gives

$$K_{d\delta} = -\frac{\rho_{lM} RT}{\sigma_{lv}} \ln \frac{P_{vd}}{P_v} - \frac{\Pi}{\sigma_{lv}} \tag{20}$$

In order to easily integrate eq 20, we assume as a crude approximation that the first term on the right-hand side is a constant

$$\frac{c}{\delta_0} = -\frac{\rho_{lM} RT}{\sigma_{lv}} \ln \frac{P_{vd}}{P_v} \tag{21}$$

The constant "c/δ_0" in eq 21 is the value of the forced increase in curvature relative to the equilibrium curvature which causes a decrease in vapor pressure for condensation at the liquid–vapor interface. The convenient constant value is partially justified by its final use for only an extremely short distance.

In essence, this pseudoequilibrium model will lead subsequently to a constant condensation rate model. Using the same techniques outlined above (for eqs 8–13) for integrating eq 20 gives eq 22 for the local dynamic angle, $\theta_{d\eta}$

$$\cos \theta_{d\eta} = 1 - \frac{1}{2b} + \frac{1}{2b\eta^2} + c(1 - \eta) \tag{22}$$

Subtracting eq 22 from eq 14 for the same value of η gives

$$\cos \theta_e - \cos \theta_{d\eta} = (1 - \eta)\frac{\rho_{lM}\delta_0 RT}{\sigma_{lv}} \ln \frac{P_{vd}}{P_v} \tag{23}$$

Although we would expect the dynamic contact angle to be a function of position and therefore film thickness, the result presented in eq 22 is partially artificial because of the assumed constant vapor pressure change in eq 21. This gives a constant curvature where $\Pi \rightarrow 0$, $K_{d\delta} = K_d$, which can be obtained using eq 20. However, we would expect that, in at least some cases at lower velocities, both K and Π would vanish as the thickness increases. Therefore, we assume a step change to $K_d = 0$ at the unknown position η_d where the contact angle reaches the apparent dynamic value θ_d. No additional change in slope occurs beyond this location in the model. In addition, we note that, since viscous effects have not been included, these equations only evaluate the effect of condensation on movement, thereby making it the controlling resistance to movement. Nevertheless, this result is found to be extremely useful below if we restrict the value of η to η_d and assume that the change $\Delta \cos \theta$ occurs over the dimensionless thickness change $(1 - \eta_d)$.

By use of interfacial kinetic theory in the form of eq 24 to relate the net mass flux of matter crossing a liquid–vapor interface[12] to the vapor pressure change from equilibrium in eq 23, $P_{vd} - P_v$, eq 25 is obtained

$$\dot{m} = C_1\left(\frac{M}{2\pi RT}\right)^{0.5}(P_{vd} - P_v) \tag{24}$$

where $\dot{m} < 0$ is the condensation rate

$$\cos \theta_e - \cos \theta_d = (1 - \eta_d)\frac{\rho_{lM}\delta_o RT}{\sigma_{lv}} \times \ln\left(1 + \frac{\dot{m}}{P_v C_l}\left[\frac{2\pi RT}{M}\right]^{0.5}\right) \tag{25}$$

The velocity can be obtained from the condensation rate using the following procedure. Since the film profile is a function of time and position, $\delta(x,t)$, the film velocity, U, at a particular film thickness is

$$U = \left(\frac{\partial x}{\partial t}\right)_\delta = \frac{-\left(\frac{\partial \delta}{\partial t}\right)_x}{\left(\frac{\partial \delta}{\partial x}\right)_t} \tag{26}$$

Using eq 27 for a condensation process which is perpendicular to the interface, gives eq 28

(26) Bankoff, S. G. *J. Phys. Chem.* **1956**, *60*, 952–955.
(27) McNutt, J. E.; Andes, G. M. *J. Chem. Phys.* **1959**, *30*, 1300–1903.

$$\frac{\left(\frac{\partial \delta}{\partial t}\right)_x}{\left(\frac{\partial \delta}{\partial x}\right)_t} = \frac{-\frac{\dot{m}}{\rho_l}\cos\theta_{d\eta}}{\tan\theta_{d\eta}} \quad (27)$$

$$U = \frac{\dot{m}}{\rho_l}(\cos\theta_{d\eta})(\cot\theta_{d\eta}) \quad (28)$$

The horizontal velocity, U, is a function of film thickness because of $\theta_{d\eta}$. However, in the following application, the ratio $U/(\cos\theta_{d\eta})(\cot\theta_{d\eta})$ is a constant. Combining eqs 25 and 28 gives the change in apparent contact angle in terms of the velocity

$$\cos\theta_e - \cos\theta_d = a_1(1-\eta_d)\ln\left[1 + \frac{a_2 U}{C_1\cos\theta_{d\eta}\cot\theta_{d\eta}}\right] \quad (29)$$

where

$$a_1 = \frac{\rho_{lM}\delta_o RT}{\sigma_{lv}}, \qquad a_2 = \frac{\rho_l}{P_v}\left[\frac{2\pi RT}{M}\right]^{0.5} \quad (30)$$

Equation 29, can be rewritten as

$$U = \frac{C_1\cos\theta_{d\eta}\cot\theta_{d\eta}}{a_2}\left[\exp\left(\frac{\cos\theta_e - \cos\theta_d}{a_1(1-\eta_d)}\right) - 1\right] \quad (31)$$

Equation 31 is compared with experimental data below. Meanwhile, for a more explicit equation, this can be expanded for small values of the exponent to give

$$U = \frac{C_1\cos\theta_{d\eta}\cot\theta_{d\eta}}{a_1 a_2(1-\eta_d)}(\cos\theta_e - \cos\theta_d)$$

$$\text{with} \qquad a_3 = |\Delta\cos\theta/a_1(1-\eta_d)| \ll 1 \quad (32)$$

For small angles, this becomes

$$U = \frac{C_1\cos\theta_{d\eta}\cot\theta_{d\eta}(\theta_d^2 - \theta_e^2)}{2a_1 a_2(1-\eta_d)}, \qquad \theta \ll 1, \quad a_3 \ll 1 \quad (33)$$

Experimentally, the velocity is measured as a function of the change in the apparent contact angle for systems with known properties a_1 and a_2. However, the value of δ_o could be difficult to estimate in some systems. The ratio $C_1/(1-\eta_d)$ is an unknown and represents a resistance which would be a function of the condensation rate. Since C_1 has a maximum ideal value of 2 and η_d, the distance over which the dynamic contact angle varies in eq 22, probably has a value of approximately 3, we presume that this ratio has a constant value of approximately −1. This is based on the assumption that the relatively low resistance to liquid flow would not allow significant curvature in the relatively thick region $\eta > 3$. Using these values and the assumption $\theta_{d\eta} = \theta_d$, eq 31 is compared with experimental data in the next section.

Comparison of Model with Data

In Figure 7, the model eq 31 is compared with the following experimental data: low velocity spreading data for octane on Teflon ($\theta_e = 26°$) and methylene iodide on nylon ($\theta_e = 41°$) obtained on flat surfaces by Schwartz and Tejada;[21] low velocity data for the capillary rise of water in a cylindrical dehydroxylated glass capillary which was initially equilibrated with water vapor for 6 h ($\theta_e = 36°$) obtained by Gribanova.[22] As demonstrated by the large velocity range evaluated for the same values of $\Delta\cos\theta$, these data represent significantly different systems. The values for the important physical properties used in the comparison are given in Table I. The hard to find vapor pressure for CH_2I_2 was obtained from ref 28. As demonstrated by eq 32 and the results in Table I, the important product a_1a_2 organizes the data. Considering the large number of assumptions associated with the development of the model and the calculations, we believe that the results demonstrate that the evaporation/condensation process has a significant effect on contact line movement. However, since the values of C_1 and η_d are currently unknown functions of the spreading velocity, a more accurate tracking of the data is not possible with this simple method. A more complete albeit much more detailed and complicated model could be developed.

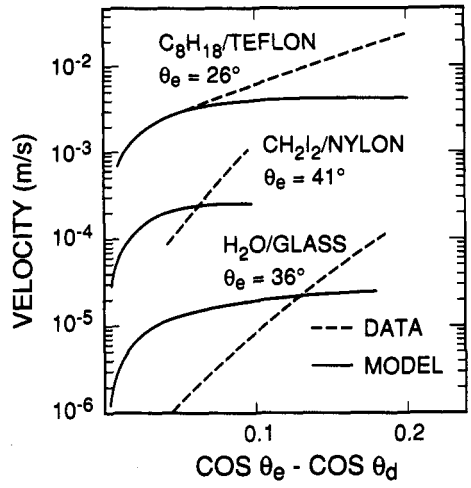

Figure 7. Comparison of eq 31 with experimental data: octane on Teflon and methylene iodide on nylon obtained on flat surfaces by Schwartz and Tejada;[19] the capillary rise of water in a dehydroxylated glass capillary obtained by Gribanova.[22]

Table I. Physical Properties for Equations 31–33 Evaluated at 293 K

system	P_v, N/m²	$10^3\sigma_{lv}$, N/m	δ_0, nm	a_2, s/m	a_1a_2, s/m
C_8H_{18}/Teflon	1391	21.8	0.16	185	19
CH_2I_2/nylon	97	51	0.16	3241	115
H_2O/glass	2327	73	5	395	3665

The value of $\delta_0 = 0.16$ nm for octane was selected based on the modeling in ref 14. The same value was used for methylene iodide because of the presumed similarity of adsorption on the plastic substrate. The value of $\delta_0 = 5$ nm for water was selected based on the comments concerning experimental data on adsorption in ref 22. We note that this additional data for water was necessary because a value of $\delta_0 = 0.16$ nm gave theoretical results that did not agree with the experimental data on velocity. This confirms the importance of adsorption to contact line motion and the fact that the adsorption isotherm for water is very complicated. No additional effort was necessary to obtain the correct velocity range in the comparison.

We find that the velocity is a function of $(a_1a_2)^{-1}$ and that Ua_1a_2 is a dimensionless velocity. This agrees qualitatively with additional data for water obtained at higher temperature by Gribanova.[22] However, the predicted velocity is found to be too large. Therefore, it appears that additional resistances to condensation and/or viscous flow are present at these higher fluxes. This is not surprising because of previously reported difficulties in measuring the ideal condensation coefficient at high

(28) Kudchadker, A. P.; Kudchadker, S. A.; Shukla, R. P.; Patnaik, P. R. *J. Phys. Chem. Ref. Data* **1979**, *8*, 499–517.

fluxes and with water generally.[29] The terms in brackets in eq 31 given the percent change in vapor pressure: for the octane/Teflon system, this is 22% for $\Delta \cos\theta = 0.054$ and 0.6% for water for $\Delta \cos\theta = 0.107$. Although the heat fluxes are large, the temperature differences are small because the conduction path is of the order 10^{-8}–10^{-9} m. The temperature field could be obtained by a two-dimensional solution of the conduction problem, which is beyond the scope of this paper. A further iteration on the solution could then be obtained by including the effect of this new temperature field on the vapor pressure using the procedures outlined in ref 12. This would also lead to a preliminary evaluation of more complex phenomena due to large temperature gradients like Marangoni flow which cannot be evaluated with the current results. However, in summary, we feel that these additional concerns would not effect the basic conclusion: evaporation/condensation could have a significant effect on contact line motion in the finite contact angle systems evaluated.

(29) Maa, J. R. *Adv. Colloid and Interface Sci.* **1983**, *18*, 227–280.

Acknowledgment. This material is based on work partially supported by the Department of Energy under Grant DE-FG02-89ER14045.A000. Any opinions, findings, and conclusions or recommendations expressed in this publication are those of the author and do not necessarily reflect the view of the DOE.